Effective and biocompatible antibacterial surfaces via facile synthesis and surface modification of peptide polymers

Ziyi Lu [a],[1], Yueming Wu [a],[1], Zihao Cong [a], Yuxin Qian [a], Xue Wu [a], Ning Shao [a], Zhongqian Qiao [a], Haodong Zhang [a], Yunrui She [a], Kang Chen [a], Hengxue Xiang [b], Bin Sun [b], Qian Yu [c], Yuan Yuan [e], Haodong Lin [d], Meifang Zhu [b], Runhui Liu [a],[e],*

[a] State Key Laboratory of Bioreactor Engineering, College of Chemistry, Chemical Engineering and Materials Science, East China University of Science and Technology, Shanghai, 200237, China
[b] State Key Laboratory for Modification of Chemical Fibers and Polymer Materials, College of Materials Science and Engineering, Donghua University, Shanghai, 201620, China
[c] Jiangsu Key Laboratory of Advanced Functional Polymers Design and Application, Soochow University, Suzhou, 215123, China
[d] Department of Orthopedic Surgery, Shanghai General Hospital, Shanghai Jiao Tong University School of Medicine, Shanghai, 200080, China
[e] Key Laboratory for Ultrafine Materials of Ministry of Education, Frontiers Science Center for Materiobiology and Dynamic Chemistry, Research Center for Biomedical Materials of Ministry of Education, School of Materials Science and Engineering, East China University of Science and Technology, Shanghai, 200237, China

ABSTRACT

It is an urgent need to tackle drug-resistance microbial infections that are associated with implantable biomedical devices. Host defense peptide-mimicking polymers have been actively explored in recent years to fight against drug-resistant microbes. Our recent report on lithium hexamethyldisilazide-initiated superfast polymerization on amino acid N-carboxyanhydrides enables the quick synthesis of host defense peptide-mimicking peptide polymers. Here we reported a facile and cost-effective thermoplastic polyurethane (TPU) surface modification of peptide polymer (DLL: BLG = 90 : 10) using plasma surface activation and substitution reaction between thiol and bromide groups. The peptide polymer-modified TPU surfaces exhibited board-spectrum antibacterial property as well as effective contact-killing ability in vitro. Furthermore, the peptide polymer-modified TPU surfaces showed excellent biocompatibility, displaying no hemolysis and cytotoxicity. In vivo study using methicillin-resistant Staphylococcus aureus (MRSA) for subcutaneous implantation infectious model showed that peptide polymer-modified TPU surfaces revealed obvious suppression of infection and great histocompatibility, compared to bare TPU surfaces. We further explored the antimicrobial mechanism of the peptide polymer-modified TPU surfaces, which revealed a surface contact-killing mechanism by disrupting the bacterial membrane. These results demonstrated great potential of the peptide-modified TPU surfaces for practical application to combat bacterial infections that are associated with implantable materials and devices.

1. Introduction

Over the past half-century, the use of implantable biomaterials and medical devices, such as catheters, pacemakers and contact lenses, has helped to diagnose, prevent and treat diseases in modern medical healthcare system. These implanted devices have restored people's health and improved their quality of life. However, implanted devices are also associated with bacterial infections, which have brought a heavy economic burden to the government and our society [1–6]. It is reported that the annual costs for healthcare-associated infections were estimated to range from 28 billion to 45 billion in the United States, and over 60% were related to medical devices [7]. Although antibiotics have been widely used to treat bacterial infections, the overuse and misuse of antibiotics contribute to the quick emergence and spread of multidrug-resistant (MDR) bacteria in clinical practice [8–13]. Conventional antibiotics have low bacterial killing efficacy on MDR

bacteria, which has severely threatened human life. Therefore, alternative strategies have been explored to fight against bacterial infections, such as antibacterial modification on materials [14–26]. In addition to antimicrobial performance, it is always an important consideration to optimize for a long-lasting antimicrobial activity, and low cytotoxicity on mammalian cells.

Host defense peptides (HDPs), which are essential components of the innate immune system, can resist microbial infection and regulate the host immune response. Since Dr. Boman isolated the first HDP from the Cecropia moth [27], a large number of natural HDPs have been identified and explored. It is generally believed that HDPs are broad-spectrum antimicrobials and are insusceptibility to drug resistance, due to their general membrane targeting mechanisms [28–32]. However, HDPs also have obvious shortcomings, such as the instability of their structure, challenges in large-quantity preparation, and the high cost of solid-phase peptide synthesis, which limit the practical application of HDPs [33]. In order to overcome the inherent drawbacks of HDPs, a growing number of HDP-mimicking polymers have been synthesized and studied [34–37]. In further study of HDP mimicking polymers, antimicrobial activities were found to be dependent on a globally amphiphilic conformation, instead of the rigid secondary structure of HDPs [34,38]. It is indicated that the flexible polymer backbone can be used to replace the peptide backbone to have an amphiphilic conformation. In order to follow the amphiphilic structure, HDP mimics such as β-peptide polymer, α-peptide polymer, poly(2-oxzoline), and poly-(-benzyl ether) have been explored [39–50]. They are broad-spectrum, biocompatible, resistant to protease, and cost-effective in synthesis. Nevertheless, it is highly desired to prevent implant-related infections rather than antimicrobial treatment after bacterial infection happens. Encouraged by the great performance of HDP mimics in solution, HDP mimics have been attached on surfaces to prevent implant-related infections [51–54]. In previous work, we demonstrated that the surface-tethered HDP mimics have excellent antimicrobial activity and biocompatibility [51]. Plasma activation was further used in the antibacterial modification of thermoplastic polyurethane (TPU) surfaces [54]. The modified surface exhibited effective antibacterial activities with long-term biocidal performance, which implied great potential in application of biomedical materials.

We also reported lithium hexamethyldisilazide (LiHMDS)-initiated superfast polymerization on amino acid *N*-carboxyanhydride (NCA) to prepare peptide polymer libraries for high-throughput functional screening of potential antibacterial peptide polymers [55–58]. We chose an racemic amino acid D,L-lysine as the monomer of the peptide polymer to increase the stability against proteolysis [59]. Among the acquired peptide polymers, peptide polymer (D,L-lysine):(γ-benzyl-L-glutamate) = 90 : 10 (DLL: BLG = 90 : 10) exhibits potent antimicrobial activity against multiple types of bacteria in solution [60]. In this study, we explore a facile and cost-effective surface modification of peptide polymer (DLL: BLG = 90 : 10) to enable material surface antibacterial properties, and further explore the antimicrobial mechanism of the surface. The peptide polymer-modified TPU (TPU-P) surfaces exhibit board-spectrum antibacterial property as well as effective contact killing ability both *in vitro* and *in vivo*.

2. Materials and methods

2.1. Materials and instrumentation

Thermoplastic Polyurethane (TPU) was purchased from Qisheng Plastic. Acridine Orange/Ethidium Bromide (AO/EB) Staining Kit and Phosphate Buffered Saline (PBS) were provided by Thermo Fisher Scientific. All of the other reagents and solvents were obtained from Shanghai Adamas Reagent. Chemicals synthesized in this work were purified using a SepaBean machine equipped with Sepaflash columns produced by Santai Technologies Inc. in China. Herein, four types of bacteria were used for *in vitro* antimicrobial test, including

Staphylococcus aureus (*S. aureus* USA 300, MRSA, methicillin-resistant *Staphylococcus aureus*), *Staphylococcus haemolyticus* (*S. haemolyticus* R01), *Escherichia coli* (*E. coli* JM109), and *Pseudomonas aeruginosa* (*P. a* 9027). *S. aureus* USA 300 LAC was utilized for *in vivo* infection assay. Human umbilical vein endothelial cells (HUVEC ATCC PCS-100-010) and NIH-3T3 fibroblast cells (3T3 ATCC CRL-1658) were obtained from the Cell Bank of Typical Culture Collection of Chinese Academy of Sciences (Shanghai, China) and were used for cytotoxicity studies. ^{1}H NMR spectra were recorded using a Bruker spectrometer at 400 MHz and D_2O was used as the solvent. ^{1}H NMR chemical shifts were referenced by the resonance of residual protonated solvent (δ 4.79 for D_2O). Gel permeation chromatography (GPC) was performed on a Waters GPC instrument equipped with a Brookhaven BI-MwA multi-angle light scattering detector (BI-MwA), a refractive index detector (Waters 2414), and a Tosoh TSKgel Alpha-2500 column (particle size 7 μm) and a Tosoh TSKgel Alpha-3000 column (particle size 7 μm) connected in series. GPC was analyzed using DMF, supplemented with 0.1 M LiBr, as the mobile phase at a flow rate of 1 mL/min at 50 °C. Relative number-average molecular weight (M_n), degree of polymerization (DP) and dispersity index (Đ) were calculated from a calibration curve using poly-methylmethacrylate (PMMA) as standards. The sample was filtered through 0.22 μm polytetrafluoroethylene (PTFE) filters before GPC analysis. The surface morphology of the TPU-P surface was obtained using a Multimode Nanoscope V scanning probe microscopy system Atomic Force Microscope (AFM) (Brucker Co., Ltd., USA). The morphology of bacteria and human red blood cells (hRBCs) on the TPU-P surface were recorded utilizing a Hitachi S-4800 Field Emission Scanning Electron Microscope (FESEM). The images of cell culture on the TPU-P surface were taken using a Nikon ECLIPSE Ti–S fluorescence microscopy.

2.2. Synthesis of the peptide polymer

Nε-*tert*-butyloxycarbonyl-D,L-lysine (Boc-D,L-Lys) NCA, and γ-benzyl-L-glutamate (BLG) NCA were prepared by following a method reported previously [55]. Boc-D,L-Lys NCA (0.9 mmol, 245.07 mg) and BLG NCA (0.1 mmol, 26.33 mg) were mixed into a dry reaction flask and then dissolved in THF (3 mL). Afterward, 2 mL of lithium hexamethyldisilazide (LiHMDS) in THF (0.1 M) was added to the reaction mixture. After stirring for 5 min, thin-layer chromatography (TLC) was used to monitor the completion of the reaction. Then 2-(tritylthio) ethanamine (0.2 mmol, 63.9 mg) was added into the reaction flask, and the reaction was stirring overnight to achieve C-terminus functionalization of the polymer. The resulting polymer was initially precipitated out as a white solid through the slow addition of cold petroleum ether (45 mL) into the reaction mixture, and then was redissolved in THF (1 mL). After two dissolution and precipitation cycles, the terminal trityl and side-chain NHBoc protected polymer was obtained and then characterized by gel permeation chromatography (GPC) using DMF (containing 0.1 M LiBr) as the mobile phase at a flow rate of 1 mL/min. To remove the protecting groups, the polymer was treated with trifluoroacetic acid (TFA) in the presence of triethylsilane (5%, v/v) under gentle shaking overnight. Afterward, TFA was removed under N_2 flow. The resulting reaction mixture was firstly dissolved in methanol (0.5 mL) and then precipitated out as a white solid through the slow addition of diethyl ether (45 mL) into the solution. After another two dissolution and precipitation cycles, the deprotected polymer was dried under a gentle N_2 flow. The final product was obtained as a TFA salt through lyophilization.

2.3. Surface modification of TPU

The purchased TPU was cut into sheets (circle, d = 1 cm) and prepared according to the literature [54]. The TPU sheets were cleaned with 2% Tween-20 (98% deionized water) under sonication for 15 min followed by deionized water and anhydrous ethanol twice for 15 min each

time. Next, the TPU sheets were dried under a gentle N_2 flow. Then the surface of the cleaned TPU sheets was activated using a plasma irradiator. Specifically, the sheets were set into the cavity and irradiated with a plasma irradiator at 70 W for 5 min on each side under an O_2 flow (0.3–0.4 MPa). After irradiation, these sheets were immersed into the functionalization reagent containing 1 : 10 bromoform: toluene (v/v) for 7–8 h to functionalize the activated TPU surfaces with brominated groups. The bromoform modified TPU sheets were washed with toluene, CH_2Cl_2, and ethanol. They were then kept in a vacuum vessel for overnight drying. The dried bromoform-modified TPU surface was incubated in an 80 µL solution of peptide polymer (DLL: BLG = 90 : 10) (1 mg/mL) in 1X degassed PBS buffer (pH 7.4, supplemented with 10% glycerol v/v) for 9–10 h. Later, an aliquot of 10 µL thioglycerol solution at 100 mg/mL in 1X degassed PBS buffer (pH 7.4, supplemented with 10% glycerol v/v) was added, and the whole mixture was incubated for another 3–4 h at room temperature. Finally, the peptide polymer-modified TPU surface (TPU-P) was cleaned by deionized water and dried under a gentle N_2 flow.

2.4. Characterization of polymer density on the TPU-P surface

The TPU-P was characterized for polymer layer thickness using ellipsometer, surface morphology using AFM, and surface hydrophilicity using contact angle meter. The grafting density of polymer chain was indirectly obtained with the formula, $\sigma = (hpNA)/M_n$, with symbol h being the thickness of polymer chain, p (assuming as 1 g/cm^3) being the density of polymer, NA being the Avogadro constant, and M_n being the number-average molecular weight of polymers in solution.

2.5. Antimicrobial assay of TPU-P

The antimicrobial ability of the TPU-P surface was tested against four bacteria, *S. aureus*, *S. haemolyticus*, *E. coli*, and *P. aeruginosa*. The bacteria suspension with a cell density at 5×10^5 CFU/mL was utilized as the working solution. TPU-P surfaces were placed into a 24-well plate, and each of the surfaces was evenly covered by 80 µL of bacterial working solution. After incubation at 37 °C for 2.5 h, 1000 µL of PBS was gently added into each well using, and then the plate was sonicated for 3 min and further vortexed for 2 min to ensure the detachment of bacteria from the surfaces.

The following formula was used to calculate the killing efficacy of the TPU-P surface against the bacteria. In order to get the colony number of the TPU-P surface C_{sample}, 30 µL of bacterial suspension was transferred from each well to an agar plate. The plate was incubated at 37 °C overnight. Bacterial suspension without incubation with any surface was used as the negative control to give the colony number $C_{control}$.

$$\text{Killing efficacy} \cdot (\%) \cdot = \frac{C_{control} - C_{sample}}{C_{control}} \cdot \times \cdot 100.$$

2.6. Leaching assay of TPU-P surface

A leaching assay was undertaken to analyze the stability of TPU-P surface. Leaching solution from TPU-P and TPU was obtained by incubating the TPU-P and the bare TPU in 1 mL of degassed PBS in a 24-well plate respectively. 3 µL of the stock fluorescamine solution (3 mg/mL in DMSO) and 27 µL of the leaching solution were added into a 384-well plate, and then the solution was uniformly mixed using a pipette. After co-incubating in the absence of light for 15 min, the fluorescence intensity of each well in the 384-well plate was recorded at Ex 365 nm and Em 470 nm. The peptide polymer solution (1 mg/mL in degassed PBS) was used as the control.

2.7. SEM characterization of bacterial morphology on the TPU-P surface

SEM was used to characterize the morphology of bacteria on the

TPU-P surface after the antimicrobial assay. After incubating bacteria on the TPU-P surface for 2.5 h, the surface was immersed in 2.5 w.t.% glutaraldehyde in phosphate buffer (0.2 M, PB, pH 7.2) at 4 °C overnight. Then the surface was gently rinsed with PBS for 3 times and dehydrated using graded ethanol (30%, 50%, 70%, 80%, 90%, 95%, 100%) for 5 min at each gradient. Finally, the sample was dried under a gentle N_2 flow and then used for characterization.

2.8. Cytoplasmic membrane permeability assay on the peptide polymer-modified Au (Au–P) surface

The Au–P surface-induced cytoplasmic membrane permeability was tested against *E. coli*. The bacteria suspension was diluted to a cell density at 10^8 CFU/mL, then 10 µL of NPN (2.1929 mg/mL in DMSO) was added into 10 mL bacterial suspension to obtain the working solution. Au–P surfaces were placed into a 24-well plate, and each of the surfaces was evenly covered by 80 µL of working solution. After incubation at 37 °C for 0.5, 1.5, and 2.5 h, 200 µL of HEPES was gently added into each well, and then the plate was sonicated for 3 min and further vortexed for 2 min to ensure the detachment of bacteria from the surface. 80 µL of the solution was pipetted into a 96-well plate to record the fluorescence intensity of each well at Ex 350 nm and Em 420 nm.

2.9. Electrical conductivity on the TPU-P surface

E. coli and MRSA were diluted to a cell density at 5×10^5 CFU/mL to obtain the working solution, respectively. TPU-P surfaces were placed into a 24-well plate, and each of the surfaces was evenly covered by 80 µL of working solution. After incubation at 37 °C for 0.5, 1, 1.5, 2 and 2.5 h, 2420 µL of PBS was gently added into each well, and then the plate was sonicated for 3 min and further vortexed for 2 min. Afterward, 2500 µL solution from each well was transferred into a centrifuge tube (15 mL), and a conductivity meter was used to measure the electrical conductivity of the solution in each tube.

2.10. Hemolysis assay on the TPU-P surface

Fresh human blood was centrifuged at 1000 rpm for 15 min and then rinsed with TBS for 3 times to get human red blood cells (hRBCs). The obtained hRBCs was diluted to 5% (v/v) suspension with TBS for further use. 50 µL of TBS was first dropped onto the TPU-P surface, and 50 µL of hRBCs was added subsequently. After incubation at 37 °C for 1 h, the suspension on the surface was collected and centrifuged at 3700 rpm for 5 min. Afterward, each well of the 96-well plate was charged with 80 µL of the suspension and the OD value was collected by a microplate reader at 405 nm.

The formula showed below was used to calculate the percentage of hemolysis relative to the Triton X-100 (TX-100) control. A_{sample}, $A_{positive}$, and $A_{negative}$ represent the OD value of the TPU-P surface, TX-100 (3.2 mg/mL) and TBS, respectively.

$$\text{Hemolysis} \cdot (\%) \cdot = \cdot \frac{A_{sample} - A_{negative}}{A_{positive} - A_{negative}} \cdot \times \cdot 100$$

2.11. SEM characterization on the morphology of hRBCs

SEM was used to characterize the morphology of hRBCs on the TPU-P surface after the hemolysis assay. The surface was immersed in 2.5 w.t.% glutaraldehyde in phosphate buffer (0.2 M, PB, pH 7.2) at 4 °C overnight. Then the surface was gently rinsed with PBS 3 times and dehydrated utilizing graded ethanol (30%, 50%, 70%, 80%, 90%, 95%, 100%) for 5 min at each gradient. Finally, the sample was dried under N_2 for SEM characterization.
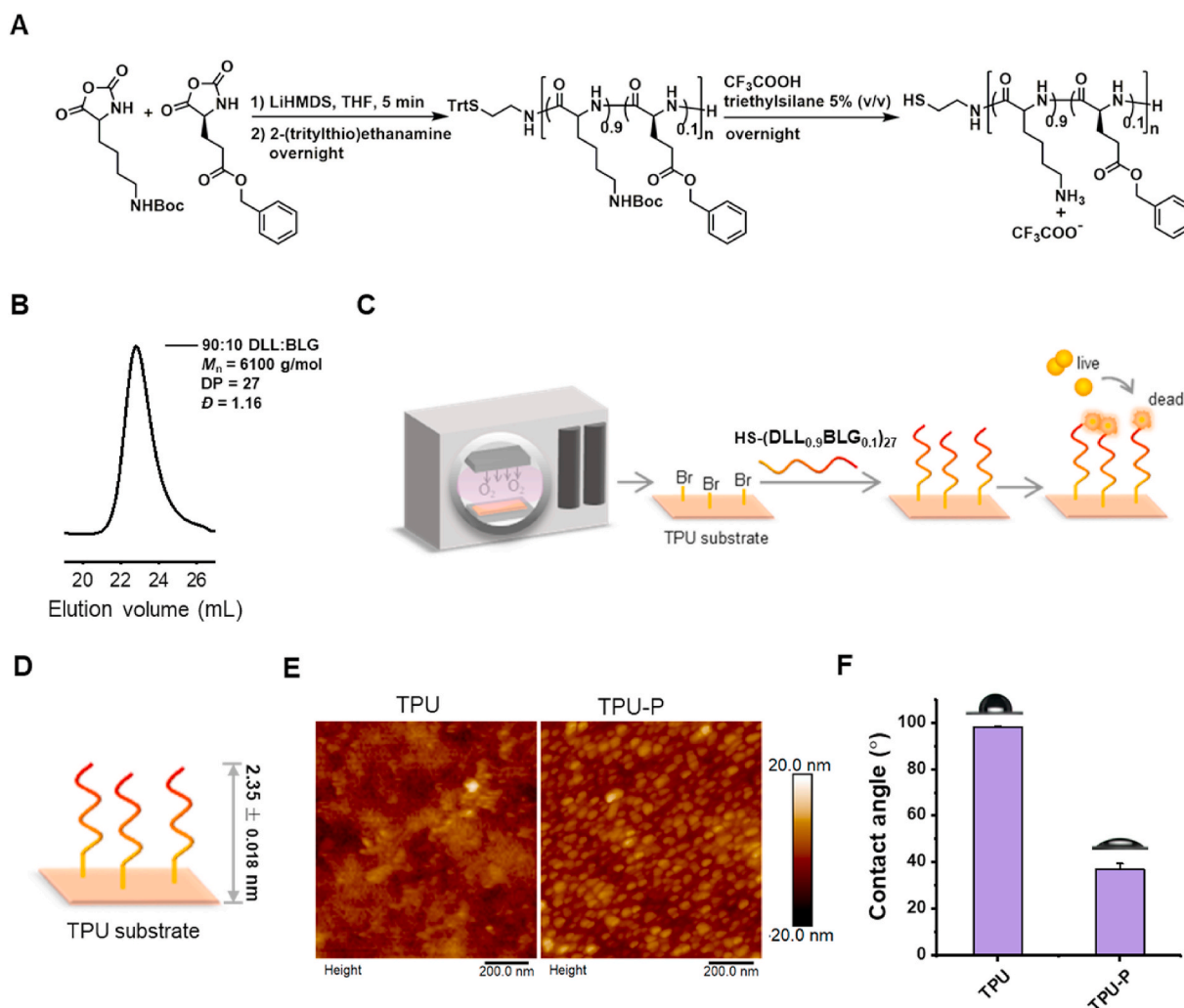
Fig. 1. (A) Synthesis of peptide polymer (DLL: BLG = 90 : 10) from the LiHMDS-initiated NCA polymerization. (B) GPC characterization of peptide polymer (DLL: BLG = 90 : 10) at the terminal and side-chain protected stage. (C) Modification of the peptide polymer-modified TPU (TPU-P) surface. (D) Ellipsometer characterization of the TPU-P surface to provide the thickness of the peptide polymer layer on TPU surface. (E) AFM characterization of the TPU-P surface and the bare TPU surface. (F) Water contact angles of the TPU-P surface and the bare TPU surface.

2.12. Cytotoxicity of the TPU-P surface

Two types of mammalian cells, human umbilical vein endothelial cells (HUVEC ATCC PCS-100-010) and NIH-3T3 fibroblast cells (3T3 ATCC CRL-1658) were cultured in TCPS petri dishes using DMEM (containing 10% FBS, 100 U/mL penicillin, 100 μg/mL streptomycin, and 2 mM L-glutamine) at 37 °C under a 5% CO2 atmosphere, respectively. Cells at 80–90% confluency were detached from the petri dish and collected and diluted in DMEM to a final concentration of 8×10^4 cell/mL. TPU-P surfaces were put in a 24-well plate, and each well was thoroughly immersed with 1 mL of cell suspension. Bare TPU surfaces were used in the same plate for comparison. After the plate was incubated at 37 °C for 24 h, the cells were stained with 20 μL 1 : 1 ratio of Acridine Orange: Ethidium Bromide (AO: EB, 12.5 μg/mL in PBS) and further incubated for 10 min in the absence of light to give green fluorescence for live cells and red fluorescence for dead cells. After removing the staining solution from the surface and washing the surface with 500 μL PBS gently, the stained cells were observed using a fluorescence microscope.

The toxicity of extracts obtained from the TPU-P surfaces was also evaluated using the elution test method. To be specific, these extracts were obtained by immersing the TPU-P surface into 1 mL of DMEM culture medium at 37 °C for 24 h. The extracts were added to a 96-well

plate of HUVEC and NIH-3T3 cells, which were pre-cultured at 37 °C for 24 h at a cell density of 8×10^4 cell/well. Then 10 μL of MTT solution (5 mg/mL) was added to each well and the plate was incubated in the absence of light for 4 h. After removing the solution in each well, 150 μL of DMSO was added and the plate was incubated at 37 °C for another 15 min. Finally, the plate was gently shaken for 10 min to dissolve the purple MTT-formazan crystals and the OD value was recorded using a microplate reader at 570 nm.

The following formula was used to calculate cell viability. A_{sample} represents the OD value of cells with the extracts from TPU-P surfaces and bare TPU surfaces; $A_{control}$ represents the OD value of cells in DMEM without extracts; the A_{blank} represents the OD value of DMEM.

$$\text{Cell} \cdot \text{viability} \cdot (\%) \cdot = \cdot \frac{A_{sample} - A_{blank}}{A_{control} - A_{blank}} \cdot \times \cdot 100$$

2.13. In vivo assay using subcutaneous implantation infection model

All animal-related procedures were approved by the Animal Care and Use Committee of Shanghai General Hospital. Pathogen-free Sprague-Dawley (SD) rats (female, 200–250 g, 8–10 weeks) were anesthetized using 1% pentobarbital sodium (50 mg/kg) through intraperitoneal injection before the operation. Excess hair on the back of the rats was shaved with a pet shaving knife, and hair removal cream
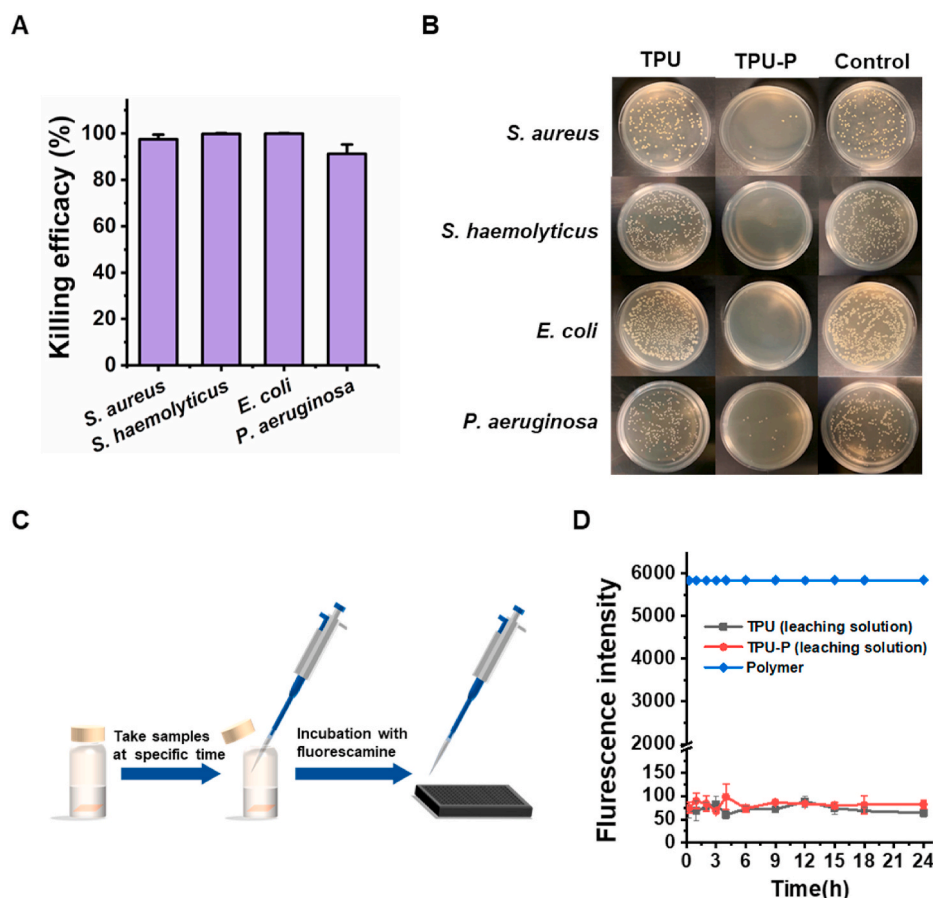
Fig. 2. (A) Antibacterial activity of the TPU-P surface against *S. aureus*, *S. haemolyticus*, *E.coli*, and *P. aeruginosa*. (B) The colony number of TPU surface, TPU-P surface and control after incubation with *S. aureus*, *S. haemolyticus*, *E.coli*, and *P. aeruginosa* for 2.5 h with necessary dilution. (C) Leaching assay utilized to evaluate the possible leaching from the TPU-P surface. (D) Fluorescence intensity measured by fluorescamine assay of leaching solution from TPU surface and TPU-P surface, and unmodified polymer solution (1 mg/mL in degassed PBS).

was applied on the back of the rats to remove the residual hair. Then the back was wiped with saline and eventually disinfected with alcohol. Both TPU-P sheets and bare TPU sheets were incubated with MRSA USA 300 LAC, and then respectively implanted into the left and the right side of the same rat's back for comparison. Freshly cultured MRSA (*S. aureus* USA 300 LAC) cells were firstly diluted into a concentration of 5×10^5 CFU/mL as the working suspension. Then an aliquot of 15 μL of MRSA suspension was evenly separated on the surface of the substrate (0.5×1 cm^2) and the whole material was incubated at 37 °C for 2.5 h. After that, the MRSA-pre-incubated substrates were implanted into the back of the rats. After 1, 3, and 7 days of implantation, the substrate-contacting upper tissues were surgically removed, homogenized, and centrifuged. The supernatant was taken out and spread onto agar plates with necessary dilution for further CFU determination.

2.14. Histocompatibility assay on subcutaneous implantation

Hematoxylin and Eosin staining (H&E staining) and gram staining were used to study the histocompatibility of TPU-P after the *in vivo* implantation study mentioned above in 2.13. After 1, 3, and 7 days of implantation, the rats were anesthetized, and then the substrate-contacting upper tissues were surgically removed and transferred into tubes filled with 4% paraformaldehyde. The fixed upper tissues were finally paraffin embedded and sectioned for H&E staining and gram staining.

3. Results and discussion

3.1. Preparation and characterization of the TPU-P surface

The peptide polymer (DLL: BLG = 90 : 10) was synthesized from the

fast ring-opening NCA polymerization on a mixture of Boc-D,L-Lys NCA and BLG NCA in 90 : 10 ratio, using LiHMDS as the initiator. The racemic D,L-Lys residues enable the peptide polymer to have great resistant to proteolysis, and the mixture of two monomers enabled the peptide polymer to have an amphiphilic structure bearing positive charges. LiHMDS initiates an extremely rapid NCA polymerization that is completed within minutes. It is superfast compares to the dominantly used primary initiators which require several days to reach completion. Furthermore, the whole process can be operated in an open vessel without any protection, which greatly facilitate the operation. The polymerization completed within 5 min, and then the obtained peptide polymer was functionalized with a C-terminal tritylthiol *in situ* (Fig. 1A). The resulting polymer was deprotected in trifluoroacetic acid to give the desired peptide polymer bearing a C-terminal thiol group with a number-average molecular weight (M_n) of 6, 100 g/mol, a chain length of 27 mer (DP = 27) and a narrow dispersity ($Đ$ = 1.16) as characterized by gel permeation chromatography (GPC) (Fig. 1B). ^{1}H NMR analysis on the final peptide polymer (H_a: H_d = 0.54 : 2) indicated that the ratio of the two amino acid subunit (DLL: BLG = 9.26 : 1) in the obtained peptide polymer was consistent with the expectation of 90 : 10 (Fig. S1).

Before peptide polymer modification, TPU sheets were activated by exposure to O$_2$ plasma with a power of 70W for 5 min, followed by treatment with bromoform to functionalize the TPU surface with bromide. The peptide polymer (DLL: BLG = 90 : 10) was then grafted to the brominated surface via the terminal thiol group of the polymer chain (Fig. 1C). The ellipsometry characterization indicated a polymer layer thickness of 2.35 ± 0.02 nm, correlating to a polymer grafting density of 0.23 chain/nm [2] (Fig. 1D). Atomic force microscopy (AFM) characterized the surface morphology of TPU-P and bare TPU surface. The roughness value of bare TPU surface was 3.23 nm. After the surface modification, the roughness value of TPU-P surface was 3.79 nm, and
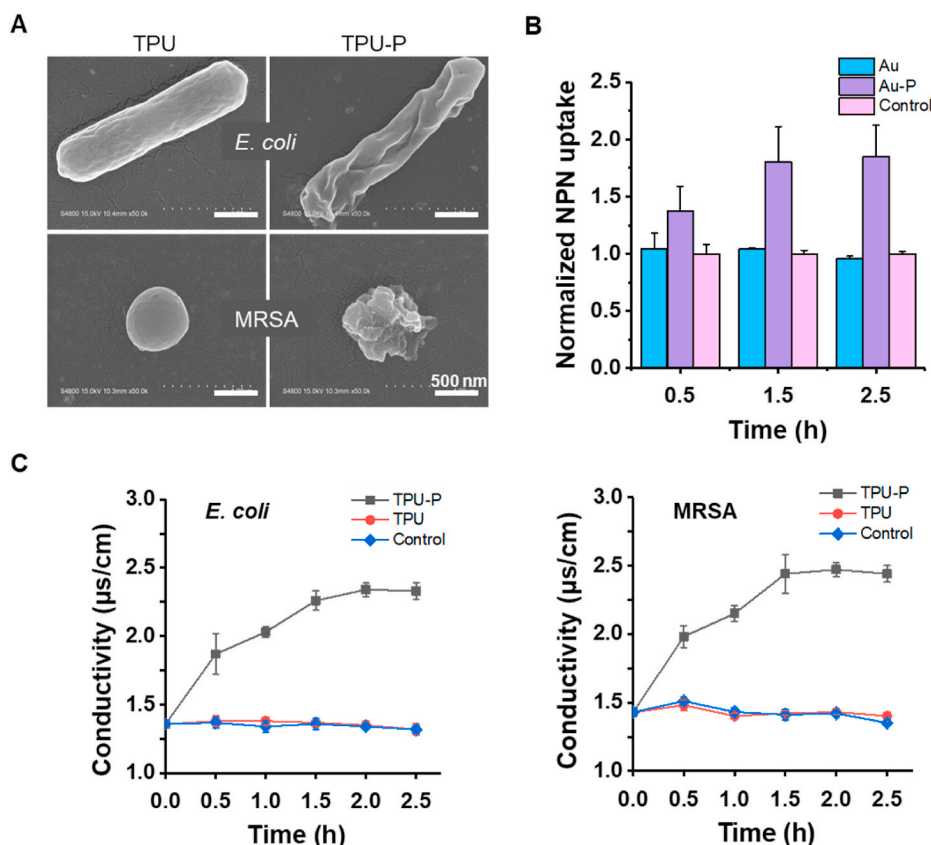
Fig. 3. (A) SEM characterization of the morphology of *E. coli* and MRSA on TPU-P surfaces after 2.5 h of incubation. Bare TPU surfaces were used as the control. (B) *E. coli* cytoplasmic membrane permeability assay induced by the peptide polymer-modified Au surface. (C) Effect of the TPU-P surface on the cellular leakage of *E. coli* and MRSA.

the morphology of the polymer could be observed, which indicated that the peptide polymer had been modified onto the TPU surface successfully (Fig. 1E). Water contact angle analysis was performed to verify the change of hydrophilicity and hydrophobicity of the TPU surface after modification with the peptide polymer. We found that the bare TPU surface was hydrophobic with the contact angle of 98°. Nevertheless, the contact angle decreased from 98° to 36.9° after the surface modification, and the hydrophilicity of the TPU surface increased substantially, which also indicates the successful surface grafting of the peptide polymer onto the TPU surface.

### 3.2. Antimicrobial activity of TPU-P surface

Once the bacteria adhere to implanted surfaces, they may cause implant-related infections. Therefore, it is necessary to evaluate the antimicrobial activities of implanted surfaces. According to Chinese Standard GBT21866-2008, the surfaces show antibacterial effect when the antibacterial rate is equal or greater than 90%. The antimicrobial activity of TPU-P was assessed against Gram-positive bacteria: *S. aureus* (MRSA) and *S. haemolyticus*, and Gram-negative bacteria: *E.coli* and *P. aeruginosa*. The killing efficacy after bacteria being exposed to TPU-P surface for 2.5 h in contact was quantified with the antimicrobial assay. TPU-P exhibited effective killing of various bacteria on contact, showing killing efficacy of 99.9% against *E. coli*, 97.5% against MRSA , 99.9% against *S. haemolyticus* and 91.2% against *P. aeruginosa,* respectively (Fig. 2A). We also photographed the colonies of bacteria on the LB ager plate according to the above results. The colonies on TPU-P surfaces were far less than those on TPU surfaces and the control (Fig. 2B). These results indicated the potent antibacterial activities and effective contact-killing ability of TPU-P on all these bacteria.

For biomedical materials and devices, stability of modified surfaces

is a great challenge. Hence, we used the fluorescamine analysis to examine the stability of the TPU-P surface to evaluate possible leaching from material surface. Fluorescamine gives fluorescent products when reacted with primary amines, so it can be used to examine the existence of polymers with primary amines in solution. Unmodified peptide polymer (DLL: BLG = 90 : 10) (1 mg/mL) solution was used as the positive control, and bare TPU was used as the negative control. The fluorescence intensity of the leaching solution was in the range of 60–90 for both TPU-P and the negative control, whereas the positive control was over 5800. This result indicates no detectable peptide polymer leaching from the modified surface, which supports above conclusion that TPU-P surfaces kill bacteria on contact (Fig. 2C and D). Overall, the TPU-P surface showed excellent contact-killing ability against both Gram-positive and Gram-negative bacteria, without leaching concerns.

3.3. Antimicrobial mechanism of TPU-P

In order to figure out the antimicrobial mechanism of the TPU-P surfaces, we did scanning electron microscopy (SEM) characterization on the morphology of bacteria. We found that untreated *E. coli* and MRSA on bare TPU surfaces had intact and smooth bacterial cell membranes, while *E. coli* and MRSA on TPU-P surfaces had shrinking and severely damage bacterial membrane (Fig. 3A).Furthermore, we explored the interaction between the peptide polymer-modified surface and the bacterial membrane of *E. coli*. We examined the permeability of the outer membrane with 1-N-phenyl-naphthylamine (NPN) as the fluorescent probe. NPN is a hydrophobic fluorescent probe for detecting damage of the outer membrane of Gram-negative bacteria. When the permeabilization of the outer membrane changed, an increased fluorescence intensity can be observed. We used Au surface as a model substrate in this assay, because the TPU substrate itself absorbed
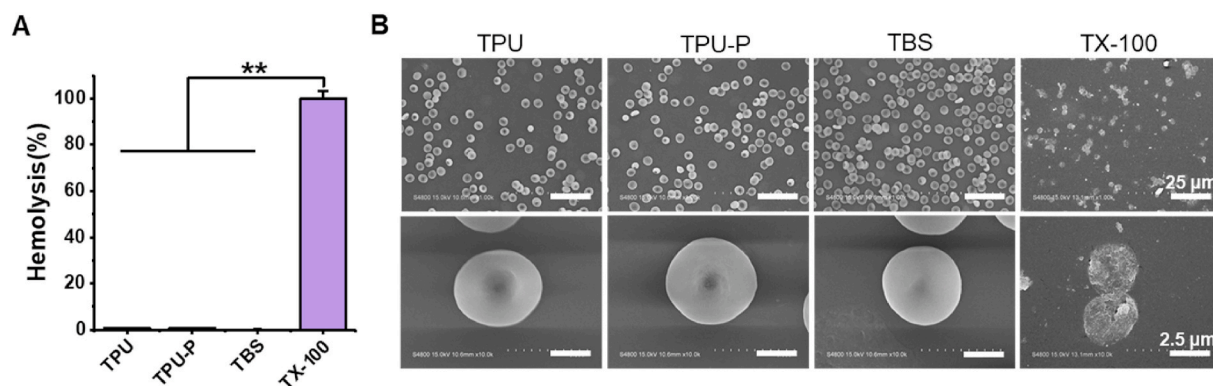
Fig. 4. Hemocompatibility study. (A) Hemolysis of the TPU-P surface towards hRBCs; (B) SEM characterization of the morphology of hRBCs after incubation with bare TPU and TPU-P surfaces, using TBS and TX-100 treated hRBCs as the negative and positive control of cell membrane damage, respectively. **p < 0.01.

fluorescent dye and affected experiment results. In our recent report, we modified the polymer to the gold surface with Au-thiol chemistry and demonstrated great antimicrobial activities [51]. We prepared the peptide polymer-modified Au (Au–P) surfaces, and found that the killing efficacy of Au–P against *E. coli* was 99.7%, similar to the TPU-P surfaces (Fig. S3). We found that the Au–P surface exhibited an obvious membrane permeabilization, while the bare Au surface and control didn't cause membrane permeabilization (Fig. 3B). We further evaluated the release of cytoplasmic materials to better define the action of the peptide polymer-modified surface on the bacterial membrane of *E. coli* and MRSA, respectively. The release of cytoplasmic materials was measured by the electrical conductivity of the bacteria suspension medium, which contacted with material surfaces. We found that the electrical conductivity kept increasing until reaching a plateau at around 2.34 µs/cm after adding the *E. coli* suspension onto the TPU-P surfaces for 2 h, and the bare TPU surfaces maintained a steady and low value at around 1.36

µs/cm. The trend of the electrical conductivity was almost the same in MRSA suspension, the electrical conductivity reached a plateau at around 2.44 µs/cm after 1.5 h, and the bare TPU surfaces maintained a steady and low value at around 1.43 µs/cm (Fig. 3C). All above results suggested that the peptide polymer-modified surfaces kill bacteria by disrupting bacterial membrane.

3.4. In vitro biocompatibility of TPU-P

In addition to potent antibacterial activity, favorable biocompatibility is also one of the essential requirements of biomedical devices. In many applications, the biomedical surface may contact with blood, so the hemolysis is always a great concern. Hence, we examined the TPU-P surface for its hemocompatibility with human red blood cells (hRBCs). TX-100 and TBS were used as the positive and negative controls, respectively. After incubating with hRBCs for 1 h, the hemolysis ratios
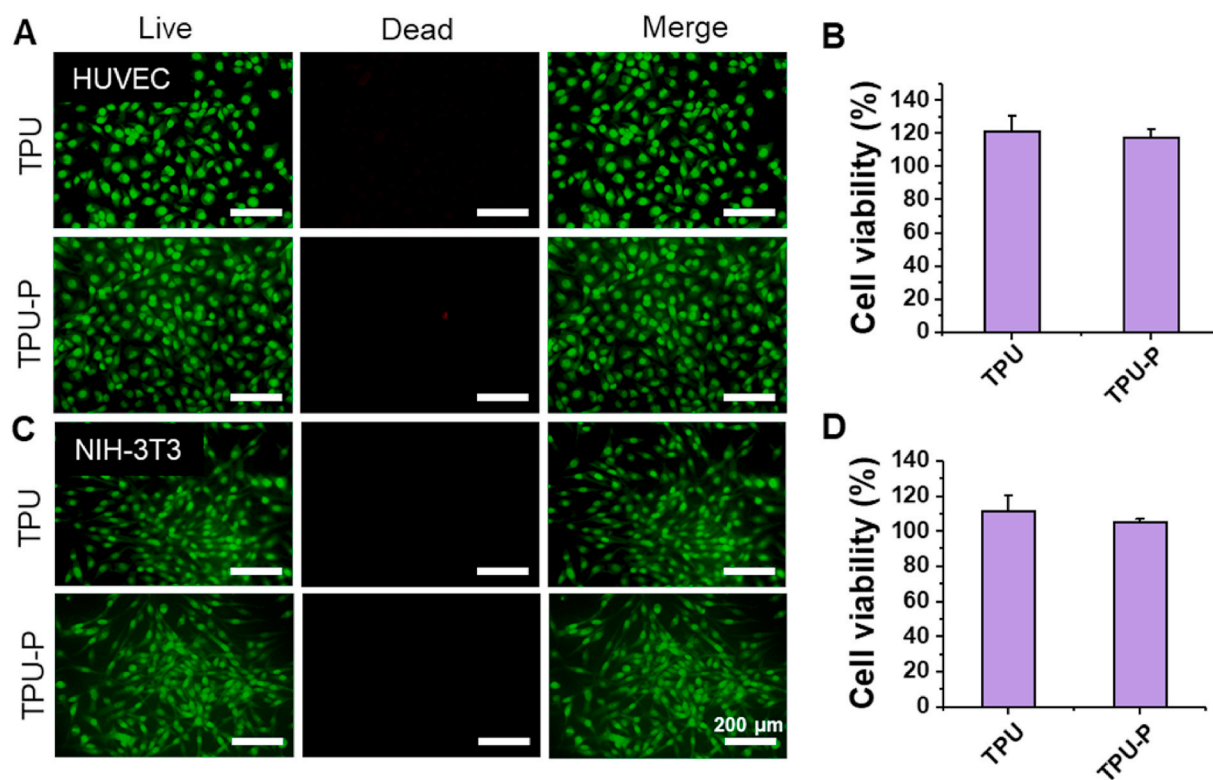
Fig. 5. Cytotoxicity studies of mammalian cells. (A, C) The proliferation of HUVEC and NIH-3T3 cells seeded on the TPU-P surfaces. The images were taken after cells were seeded on the TPU and TPU-P surfaces for 24 h and then stained with AO (green fluorescence, living cells)/EB (red fluorescence, dead cells). (B) MTT assay to evaluate the cell viability of HUVEC and (D) NIH-3T3 on bare TPU and TPU-P surfaces, respectively.
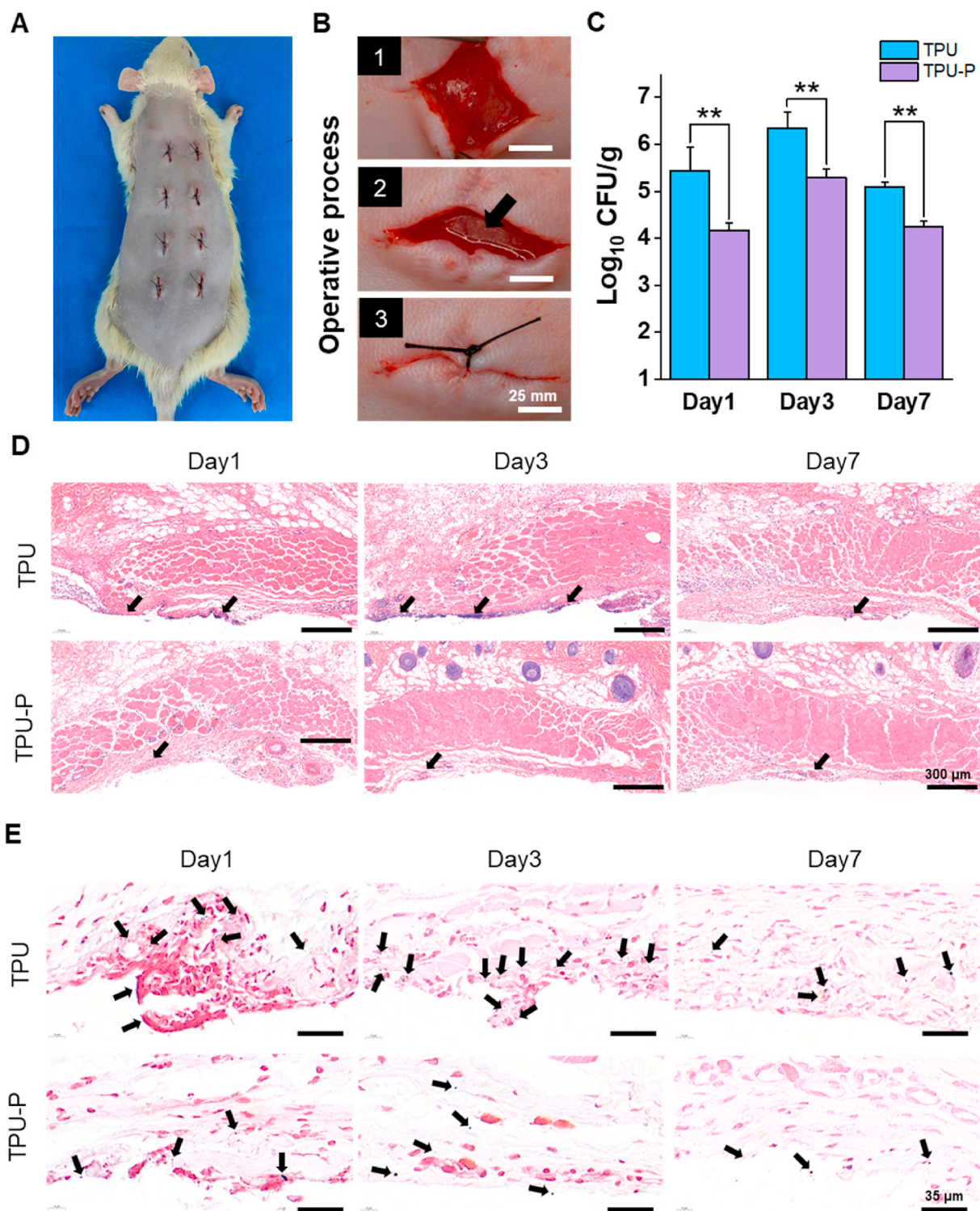
Fig. 6. *In vivo* subcutaneous implantation infection study using MRSA-pre-incubated TPU and TPU-P substrates. (A) *In vivo* subcutaneous implantation infection model. (B) Illustration of the procedure of subcutaneous implantation, with the arrow points to implanted TPU. (C) *In vivo* antimicrobial activities of TPU-P after 1 day, 3 days, and 7 days of implantation, using bare TPU as the control for comparison. (D) Histological analysis on contacting tissues stained with H&E on day 1, day 3 and day 7 after subcutaneous implantation. Arrows point to inflammatory cells. (E) Histological analysis on implant-contacting tissues with gram staining on day 1, day 3 and day 7 after subcutaneous implantation. MRSA in the contacting tissue were stained violet after the gram staining. **p < 0.01.

are 0.54% and 0.56% for TPU-P and bare TPU, respectively (Fig. 4A). TPU-P surfaces displayed an excellent biocompatibility with negligible hemolysis, similar to bare TPU surfaces. A further SEM characterization showed healthy morphology of hRBCs with smooth cell membrane on both bare TPU surfaces and TPU-P surfaces, similar to the TBS control. In sharp contrast, the morphology of TX-100 treated hRBCs was severely damaged (Fig. 4B). This observation indicates the outstanding hemocompatibility of the TPU-P surfaces.

Furthermore, cytotoxicity on mammalian cells is another concern for biomedical devices. We examined the possible cytotoxicity of TPU-P

surfaces with human umbilical vein endothelial cells (HUVEC) and NIH-3T3 fibroblast cells, which are two types of representative mammalian cells. A direct contact assay between TPU-P and HUVEC/fibroblast cells was employed to investigate the cytotoxicity of TPU-P surface. After HUVEC and fibroblast cells were cultured on TPU-P and bare TPU surfaces for 24 h, acridine orange/ethidium bromide (AO/EB) were used for live-dead staining. Cells on both TPU-P and TPU surfaces exhibited healthy cell morphology with negligible cell death (Fig. 5A, C). We also performed a quantitative viability assay using MTT to further evaluate the possible cytotoxicity on the soaking solution of TPU-P, and found no cytotoxicity towards HUVEC and fibroblast cells (Fig. 5B, D). Overall, TPU-P surface exhibited remarkable biocompatibility with negligible hemolysis and cytotoxicity *in vitro*, indicating a promising application in biomedical devices.

3.5. In vivo subcutaneous implantation infection assay

A large number of implant-related infections resulted from the poor infection prevention in clinical applications. Therefore, the *in vivo* antimicrobial efficacy is essential for preventing implant-related infections. Due to the potent antimicrobial activity and excellent biocompatibility of TPU-P surfaces *in vitro*, we further explored the *in vivo* antibacterial efficacy using a rat subcutaneous implantation infection model. In this study, bare TPU and TPU-P substrates (1×0.5 cm^2) were incubated with MRSA (*S. aureus* USA 300 LAC) and then were implanted into the incisions on both sides of a rat's back (Fig. 6A and B). After 1, 3, and 7 days of implantation, the substrate-contacting upper tissues were collected and homogenated to count bacterial colony. On day 1 post implantation, bare TPU control had a MRSA density of $10^{5.44}$ CFU per gram tissue, which indicated the infections of the upper tissues contacting the surfaces; whereas, TPU-P surfaces showed a 1.27 log reduction on MRSA density, which indicated an efficient alleviation on the implant-related infections. In the followed up *in vivo* studies, the TPU-P still exhibited great antibacterial activities with a 1.04 log and 0.85 log reduction compared to bare TPU control in day 3 and day 7, which implied the promising of TPU-P surfaces in maintaining a consistent antimicrobial performance over a period of time (Fig. 6C).

To further evaluate the *in vivo* antibacterial performance of TPU-P, histological analyses of the upper tissues after 1, 3, and 7 days of implantation were performed. We analyzed the inflammatory response of the upper tissues contacting the slides in above study, using hematoxylin and eosin (H&E) staining after 1, 3, and 7 days of implantation. The bare TPU control showed a severe inflammatory response after 1 and 3 days of implantation, and the inflammation response slightly diminished after 7 days. In sharp contrast, the TPU-P surfaces showed only a slight inflammatory response after 1, 3, and 7 days of implantation, which represents a substantially reduced inflammatory response compared to the bare TPU surfaces and supports the effective antibacterial property of the TPU-P surfaces (Fig. 6D). Furthermore, We used gram staining to characterize the distribution of MRSA in the substrate-contacting upper tissues. As Gram-positive bacteria, MRSA are stained violet after staining in the contacting tissues. The bare TPU control showed an obvious distribution of MRSA after 1 and 3 days of implantation, and slightly diminished after 7 days. The TPU-P surfaces showed substantially reduced density of MRSA after 1, 3, and 7 days of implantation compared to the bare TPU group (Fig. 6E). These *in vivo* data imply that the peptide polymer-modified antibacterial surfaces have great potential in developing implantable biomedical materials and devices, which can prevent or alleviate implant-associated infections.

4. Conclusions

In this study, we establish a facile and cost-effective antibacterial modification on material surfaces utilizing LiHMDS-initiated fast NCA polymerization for peptide polymer synthesis coupled with via surface plasma activation. TPU surfaces modified with the HDP-mimicking peptide polymer (DLL: BLG = 90 : 10) show potent antibacterial activity against both Gram-positive and Gram-negative bacteria. Additionally, the modified surfaces display remarkable biocompatibility with negligible hemolysis and cytotoxicity *in vitro*. These surfaces also display effective antibacterial activity and excellent histocompatibility *in vivo*. The overall performance of the peptide polymer-modified TPU surfaces, the fast synthesis of peptide polymer from LiHMDS-initiated NCA polymerization, and convenient surface modification strategy via plasma activation altogether imply the potential application of this study in dealing with surface-associated bacterial infections for implantable biomedical devices and tissue engineering scaffolds.

CRediT authorship contribution statement

Ziyi Lu: Conceptualization, Formal analysis, Validation, Writing – original draft. **Yueming Wu:** Methodology, Writing – original draft. **Zihao Cong:** Investigation, Formal analysis. **Yuxin Qian:** Investigation, Formal analysis. **Xue Wu:** Writing – review & editing. **Ning Shao:** Investigation, Formal analysis. **Zhongqian Qiao:** Investigation, Formal analysis. **Haodong Zhang:** Investigation, Formal analysis. **Yunrui She:** Visualization. **Kang Chen:** Investigation, Formal analysis. **Hengxue Xiang:** Funding acquisition, Writing – review & editing. **Bin Sun:** Funding acquisition, Writing – review & editing. **Qian Yu:** Funding acquisition, Writing – review & editing. **Yuan Yuan:** Writing – review & editing, Resources. **Haodong Lin:** Resources, Funding acquisition, Writing – review & editing. **Meifang Zhu:** Funding acquisition, Writing – review & editing. **Runhui Liu:** Conceptualization, Supervision, Project administration, Writing – review & editing.

Declaration of competing interest

The authors declare the following competing financial interest(s): R. L. and Y.W. are co-inventors on a patent covering reported antibacterial surfaces that were modified with peptide polymers. All remaining authors declare no competing interests.

Acknowledgement

Appendix A. Supplementary data

Supplementary data to this article can be found online at https://doi.org/10.1016/j.bioactmat.2021.05.008.

References

[1] K.G. Neoh, M. Li, E.T. Kang, E. Chiong, P.A. Tambyah, Surface modification strategies for combating catheter-related complications: recent advances and challenges, J. Mater. Chem. B 5 (2017) 2045–2067.

[2] A.S. Lynch, G.T. Robertson, Bacterial and fungal biofilm infections, Annu. Rev. Med. 59 (2008) 415–428.

[3] V. Nandakumar, S. Chittaranjan, V.M. Kurian, M. Doble, Characteristics of bacterial biofilm associated with implant material in clinical practice, Polym. J. 45 (2013) 137–152.

[4] D. Alves, M. Olivia Pereira, Mini-review: antimicrobial peptides and enzymes as promising candidates to functionalize biomaterial surfaces, Biofouling 30 (2014) 483–499.

[5] C.E. Edmiston Jr., C.J. Krepel, R.M. Marks, P.J. Rossi, J. Sanger, M. Goldblatt, M. B. Graham, S. Rothenburger, J. Collier, G.R. Seabrook, Microbiology of explanted suture segments from infected and noninfected surgical patients, J. Clin. Microbiol. 51 (2013) 417–421.

[6] L. Chen, H. Bai, J. Xu, S. Wang, X. Zhang, Supramolecular porphyrin photosensitizers: controllable disguise and photoinduced activation of antibacterial behavior, ACS Appl. Mater. Interfaces 9 (2017) 13950–13957.

[7] S.S. Magill, J.R. Edwards, W. Bamberg, Z.G. Beldavs, G. Dumyati, M.A. Kainer, R. Lynfield, M. Maloney, L. McAllister-Hollod, J. Nadle, S.M. Ray, D.L. Thompson, L.E. Wilson, S.K. Fridkin, Emerging infect program, multistate point- prevalence survey of health care-associated infections, N. Engl. J. Med. 370 (2014) 1198–1208.

[8] E.D. Brown, G.D. Wright, Antibacterial drug discovery in the resistance era, Nature 529 (2016) 336–343.

[9] S. Santajit, N. Indrawattana, Mechanisms of antimicrobial resistance in ESKAPE pathogens, BioMed Res. Int. 2016 (2016), 2475067.

[10] M.M. Konai, J. Haldar, Fatty acid comprising lysine conjugates: anti-MRSA agents that display in vivo efficacy by disrupting biofilms with No resistance development, Bioconjugate Chem. 28 (2017) 1194–1204.

[11] M.A. Gelman, B. Weisblum, D.M. Lynn, S.H. Gellman, Biocidal activity of polystyrenes that are cationic by virtue of protonation, Org. Lett. 6 (2004) 557–560.

[12] G. Taubes, The bacteria fight back, Science 321 (2008) 356–361.

[13] S. Wang, Y. Gao, Q. Jin, J. Ji, Emerging antibacterial nanomedicine for enhanced antibiotic therapy, Biomater. Sci. 8 (2020) 6825–6839.

[14] S. Ghosh, R. Mukherjee, D. Basak, J. Haldar, One-step curable, covalently immobilized coating for clinically relevant surfaces that can kill bacteria, fungi, and influenza virus, ACS Appl. Mater. Interfaces 12 (2020) 27853–27865.

[15] Y. Zhang, K. Hu, X. Xing, J. Zhang, M.R. Zhang, X. Ma, R. Shi, L. Zhang, Smart titanium coating composed of antibiotic conjugated peptides as an infection-responsive antibacterial agent, Macromol. Biosci. 21 (2021), e2000194.

[16] T. Wei, Q. Yu, H. Chen, Responsive and synergistic antibacterial coatings: fighting against bacteria in a smart and effective way, Adv. Healthc. Mater. 8 (2019), e1801381.

[17] Y.Q. Zhao, Y. Sun, Y. Zhang, X. Ding, N. Zhao, B. Yu, H. Zhao, S. Duan, F.J. Xu, Well-defined gold nanorod/polymer hybrid coating with inherent antifouling and photothermal bactericidal properties for treating an infected hernia, ACS Nano 14 (2020) 2265–2275.

[18] J. Song, H. Liu, M. Lei, H. Tan, Z. Chen, A. Antoshin, G.F. Payne, X. Qu, C. Liu, Redox-channeling polydopamine-ferrocene (PDA-Fc) coating to confer context-dependent and photothermal antimicrobial activities, ACS Appl. Mater. Interfaces 12 (2020) 8915–8928.

[19] Y. He, X. Wan, K. Xiao, W. Lin, J. Li, Z. Li, F. Luo, H. Tan, J. Li, Q. Fu, Anti-biofilm surfaces from mixed dopamine-modified polymer brushes: synergistic role of cationic and zwitterionic chains to resist staphyloccocus aureus, Biomater. Sci. 7 (2019) 5369–5382.

[20] S.K.R. Pillai, S. Reghu, Y. Vikhe, H. Zheng, C.H. Koh, M.B. Chan-Park, Novel antimicrobial coating on silicone contact lens using glycidyl methacrylate and polyethyleneimine based polymers, Macromol. Rapid Commun. 41 (2020) 10.

[21] Z. Ye, X. Zhu, I. Mutreja, S.K. Boda, N.G. Fischer, A. Zhang, C. Lui, Y. Qi, C. Aparicio, Biomimetic mineralized hybrid scaffolds with antimicrobial peptides, Bioact. Mater. 6 (2021) 2250–2260.

[22] J. Sun, H. Tan, H. Liu, D. Jin, M. Yin, H. Lin, X. Qu, C. Liu, A reduced polydopamine nanoparticle-coupled sprayable PEG hydrogel adhesive with anti-infection activity for rapid wound sealing, Biomater. Sci. 8 (2020) 6946–6956.

[23] Y. Zhang, X. Zhang, Y.Q. Zhao, X.Y. Zhang, X. Ding, X. Ding, B. Yu, S. Duan, F. J. Xu, Self-adaptive antibacterial surfaces with bacterium-triggered antifouling-bactericidal switching properties, Biomater. Sci. 8 (2020) 997–1006.

[24] D. Wang, M. Haapasalo, Y. Gao, J. Ma, Y. Shen, Antibiofilm peptides against biofilms on titanium and hydroxyapatite surfaces, Bioact. Mater. 3 (2018) 418–425.

[25] A.C. Engler, N. Wiradharma, Z.Y. Ong, D.J. Coady, J.L. Hedrick, Y.Y. Yang, Emerging trends in macromolecular antimicrobials to fight multi-drug-resistant infections, Nano Today 7 (2012) 201–222.

[26] H. Yu, L. Liu, X. Li, R.T. Zhou, S.J. Yan, C.S. Li, S.F. Luan, J.H. Yin, H.C. Shi, Fabrication of polylysine based antibacterial coating for catheters by facile electrostatic interaction, Chem. Eng. J. 360 (2019) 1030–1041.

[27] H.G. Boman, Antibacterial peptides: basic facts and emerging concepts, J. Intern. Med. 254 (2003) 197–215.

[28] M. Zasloff, Antimicrobial peptides of multicellular organisms, Nature 415 (2002) 389–395.

[29] M. Mahlapuu, J. Hakansson, L. Ringstad, C. Bjorn, Antimicrobial peptides: an emerging category of therapeutic agents, Front. Cell. Infect. Microbiol. 6 (2016) 194.

[30] J.M. Ageitos, A. Sanchez-Perez, P. Calo-Mata, T.G. Villa, Antimicrobial peptides (AMPs): ancient compounds that represent novel weapons in the fight against bacteria, Biochem. Pharmacol. 133 (2017) 117–138.

[31] J.J. Chen, Y.C. Zhu, M.H. Xiong, G.S. Hu, J.Z. Zhan, T.J. Li, L. Wang, Y.J. Wang, Antimicrobial titanium surface via click-immobilization of peptide and its in vitro/vivo activity, ACS Biomater. Sci. Eng. 5 (2019) 1034–1044.

[32] J.A.F. Corrêa, A.G. Evangelista, T.d.M. Nazareth, F.B. Luciano, Fundamentals on the molecular mechanism of action of antimicrobial peptides, Materialia 8 (2019), 100494.

[33] R.E. Hancock, H.G. Sahl, Antimicrobial and host-defense peptides as new anti-infective therapeutic strategies, Nat. Biotechnol. 24 (2006) 1551–1557.

[34] E.A. Porter, X. Wang, H.-S. Lee, B. Weisblum, S.H. Gellman, Non-haemolytic β-amino-acid oligomers, Nature 404 (2000), 565-565.

[35] D.H. Liu, W.F. DeGrado, De novo design, synthesis, and characterization of antimicrobial beta-peptides, J. Am. Chem. Soc. 123 (2001) 7553–7559.

[36] M.A. Schmitt, B. Weisblum, S.H. Gellman, Unexpected relationships between structure and function in alpha,beta-peptides: antimicrobial foldamers with heterogeneous backbones, J. Am. Chem. Soc. 126 (2004) 6848–6849.

[37] N.P. Chongsiriwatana, J.A. Patch, A.M. Czyzewski, M.T. Dohm, A. Ivankin, D. Gidalevitz, R.N. Zuckermann, A.E. Barron, Peptoids that mimic the structure, function, and mechanism of helical antimicrobial peptides, Proc. Natl. Acad. Sci. U. S. A. 105 (2008) 2794–2799.

[38] T.L. Raguse, E.A. Porter, B. Weisblum, S.H. Gellman, Structure−Activity studies of 14-helical antimicrobial β-peptides: probing the relationship between conformational stability and antimicrobial potency, J. Am. Chem. Soc. 124 (2002) 12774–12785.

[39] C. Ge, H. Ye, F. Wu, J. Zhu, Z. Song, Y. Liu, L. Yin, Biological applications of water-soluble polypeptides with ordered secondary structures, J. Mater. Chem. B 8 (2020) 6530–6547.

[40] K. Kuroda, W.F. DeGrado, Amphiphilic polymethacrylate derivatives as antimicrobial agents, J. Am. Chem. Soc. 127 (2005) 4128–4129.

[41] M. Zhou, X. Xiao, Z. Cong, Y. Wu, W. Zhang, P. Ma, S. Chen, H. Zhang, D. Zhang, D. Zhang, X. Luan, Y. Mai, R. Liu, Water-Insensitive synthesis of poly-beta-peptides with defined architecture, Angew Chem. Int. Ed. Engl. 59 (2020) 7240–7244.

[42] M. Zhou, M. Zheng, J. Cai, Small molecules with membrane-active antibacterial activity, ACS Appl. Mater. Interfaces 12 (2020) 21192–21199.

[43] X. Xiao, S. Zhang, S. Chen, Y. Qian, J. Xie, Z. Cong, D. Zhang, J. Zou, W. Zhang, Z. Ji, R. Cui, Z. Qiao, W. Jiang, Y. Dai, Y. Wang, X. Shao, Y. Sun, J. Xia, J. Fei, R. Liu, An alpha/beta chimeric peptide molecular brush for eradicating MRSA biofilms and persister cells to mitigate antimicrobial resistance, Biomater. Sci. 8 (2020) 6883–6889.

[44] S.J. Lam, N.M. O'Brien-Simpson, N. Pantarat, A. Sulistio, E.H. Wong, Y.Y. Chen, J. C. Lenzo, J.A. Holden, A. Blencowe, E.C. Reynolds, G.G. Qiao, Combating multidrug-resistant Gram-negative bacteria with structurally nanoengineered antimicrobial peptide polymers, Nat. Microbiol. 1 (2016), 16162.

[45] R.W. Scott, G.N. Tew, Mimics of host defense proteins; strategies for translation to therapeutic applications, Curr. Top. Med. Chem. 17 (2017) 576–589.

[46] H. Etayash, Y. Qian, D. Pletzer, Q. Zhang, J. Xie, R. Cui, C. Dai, P. Ma, F. Qi, R. Liu, R.E.W. Hancock, Host defense peptide-mimicking amphiphilic beta-peptide polymer (Bu:DM) exhibiting anti-biofilm, immunomodulatory, and in vivo anti-infective activity, J. Med. Chem. 63 (2020) 12921–12928.

[47] H. Yu, S. Yu, H. Qiu, P. Gao, Y. Chen, X. Zhao, Q. Tu, M. Zhou, L. Cai, N. Huang, K. Xiong, Z. Yang, Nitric oxide-generating compound and bio-clickable peptide mimic for synergistic tailoring surface anti-thrombogenic and anti-microbial dual-functions, Bioact. Mater. 6 (2021) 1618–1627.

[48] Y. Zhang, Q. Yin, H. Lu, H. Xia, Y. Lin, J. Cheng, PEG-polypeptide dual brush block copolymers: synthesis and application in nanoparticle surface PEGylation, ACS Macro Lett. 2 (2013) 809–813.

[49] R. Liu, X. Chen, S. Chakraborty, J.J. Lemke, Z. Hayouka, C. Chow, R.A. Welch, B. Weisblum, K.S. Masters, S.H. Gellman, Tuning the biological activity profile of antibacterial polymers via subunit substitution pattern, J. Am. Chem. Soc. 136 (2014) 4410–4418.

[50] R. Liu, X. Chen, Z. Hayouka, S. Chakraborty, S.P. Falk, B. Weisblum, K.S. Masters, S.H. Gellman, Nylon-3 polymers with selective antifungal activity, J. Am. Chem. Soc. 135 (2013) 5270–5273.

[51] Y. Qian, F. Qi, Q. Chen, Q. Zhang, Z. Qiao, S. Zhang, T. Wei, Q. Yu, S. Yu, Z. Mao, C. Gao, Y. Ding, Y. Cheng, C. Jin, H. Xie, R. Liu, Surface modified with a host defense peptide-mimicking beta-peptide polymer kills bacteria on contact with high efficacy, ACS Appl. Mater. Interfaces 10 (2018) 15395–15400.

[52] Q. Gao, T. Feng, D. Huang, P. Liu, P. Lin, Y. Wu, Z. Ye, J. Ji, P. Li, W. Huang, Antibacterial and hydroxyapatite-forming coating for biomedical implants based on polypeptide-functionalized titania nanospikes, Biomater. Sci. 8 (2019) 278–289.

[53] Z. Yang, X. Zhao, R. Hao, Q. Tu, X. Tian, Y. Xiao, K. Xiong, M. Wang, Y. Feng, N. Huang, G. Pan, Bioclickable and mussel adhesive peptide mimics for engineering vascular stent surfaces, Proc. Natl. Acad. Sci. U. S. A. 117 (2020) 16127–16137.

[54] F. Qi, Y. Qian, N. Shao, R. Zhou, S. Zhang, Z. Lu, M. Zhou, J. Xie, T. Wei, Q. Yu, R. Liu, Practical preparation of infection-resistant biomedical surfaces from antimicrobial beta-peptide polymers, ACS Appl. Mater. Interfaces 11 (2019) 18907–18913.

[55] Y. Wu, D. Zhang, P. Ma, R. Zhou, L. Hua, R. Liu, Lithium hexamethyldisilazide initiated superfast ring opening polymerization of alpha-amino acid N-carboxyanhydrides, Nat. Commun. 9 (2018) 5297.

[56] J. Ding, Glovebox free and rapid ring-opening polymerization of α-amino acid N-carboxyanhydrides in open-vessels, J. Funct. Polym. 32 (2019) 120–122.

[57] S. Luan, Facile preparation of polypeptides: moisture insensitive and superfast ring opening polymerization of N-carboxyanhydrides, Mater. Rep. 50 (2019) 99–101.

[58] X.H. Wan, X.H. Wang, Catalytic system for superfast polypeptide synthesis under atmosphere condition, Acta Polym. Sin. 50 (2019) 99–101.

[59] J. Lu, H. Xu, J. Xia, J. Ma, J. Xu, Y. Li, J. Feng, D- and unnatural amino acid substituted antimicrobial peptides with improved proteolytic resistance and their proteolytic degradation characteristics, Front. Microbiol. 11 (2020).

[60] W. Jiang, X. Xiao, Y. Wu, W. Zhang, Z. Cong, J. Liu, S. Chen, H. Zhang, J. Xie, S. Deng, M. Chen, Y. Wang, X. Shao, Y. Dai, Y. Sun, J. Fei, R. Liu, Peptide polymer

displaying potent activity against clinically isolated multidrug resistant
Pseudomonas aeruginosa in vitro and in vivo, Biomater. Sci. 8 (2020) 739–745.